Computational Modeling of Mass Transport and Its Relation to Cell Behavior in Tissue Engineering Constructs

Dennis Lambrechts, Jan Schrooten, Tom Van de Putte and Hans Van Oosterwyck

Abstract Effective recapitulation of extracellular matrix properties into a Tissue Engineering strategy is strongly involved with the need for a proper transport environment. Consumption and production of soluble medium components gives rise to gradients which influence cell behavior in various ways. Understanding how transport related phenomena can shape these gradients is targeted in this chapter by the combined use of experiments and mathematical modeling. An overview of different models is given that describe solute transport and its relation to specific cell behavior. From the simulation results important information can be extracted which help to unravel mechanisms that drive solute transport. Finally we describe the genuine efforts that have been taken to translate this information into real tissue engineering setups (e.g., optimization of culture conditions and controlled-release of growth factors).

D. Lambrechts (✉) · J. Schrooten
Department of Metallurgy and Materials Engineering, KU Leuven, Kasteelpark Arenberg 44-box 2450, 3001 Leuven, Belgium
e-mail: Dennis.Lambrechts@mech.kuleuven.be

D. Lambrechts · J. Schrooten · H. Van Oosterwyck
Prometheus, Division of Skeletal Tissue Engineering Leuven, KU Leuven, Herestraat 49-box 813, 3000 Leuven, Belgium

T. Van de Putte
TiGenix NV, Haasrode Researchpark 1724, Romeinse straat 12 box 2, 3001 Leuven, Belgium

H. Van Oosterwyck
Biomechanics Section, KU Leuven, Celestijnenlaan 300C-box 2419, 3001 Leuven, Belgium

Stud Mechanobiol Tissue Eng Biomater (2013) 10: 85–105
DOI: 10.1007/8415_2012_139

Published Online: 7 June 2012

1 Introduction

The functionality of extracellular matrix (ECM) in organ tissues is much broader than just structural support for cells that reside within. Cells are able to interact with ECM, both biochemically and biophysically, from structural remodeling induced by cell proteolytic activity [72] to stem cell lineage specification via straining of linked proteins [30]. The ECM also provides an important storage space for signaling molecules, a feature which appeared to be crucial in tissue morphogenesis [61, 121]. Morphogenesis is mainly driven by the gradients in signaling molecules (i.e. morphogens) which can arise from differences in morphogen diffusivity [79, 127] or from interstitial fluid flow-induced asymmetry in morphogen distribution upon enzymatic release from the matrix [50]. Understanding the mass transport principles which underlie the formation and maintenance of morphogen gradients is therefore fundamental to understand how these gradients will direct tissue patterning.

It should be clear that recapitulating fundamental ECM properties in a tissue engineering (TE) context relates closely to the aim of establishing a proper mass transport environment. From basic nutrients to signaling molecules, concentration gradients might exist for any soluble medium component that is consumed or produced by the cells [42]. The effects they can elicit on cell behavior are numerous and have proven to be a function of absolute concentrations, the range of operation and slope [46]. To measure such gradients, the use of biosensors [1] and tracer molecules [127] has been previously reported. Experimental quantification is however not always straightforward and can even become too challenging for more complex (in vivo-like) setups. A powerful tool that makes quantification easier and can predict gradient magnitudes for the even most complex situations [86], lies in the combined use of experiments and mathematical modeling [24].

Mathematical models help in establishing relations and insights between evolving solute profiles and specific cell behavior [80]. Such models have proven their applicability in unraveling important mechanisms and dynamics of experimental observations [25, 37]. Their usability ranges from the establishment of numerical interactions between influencing parameters [130] to optimization of culture conditions for nutrient transport [111] and modeling-based TE carrier design [16].

In light of the design of biomaterial carriers, special attention should be attributed to the environmental remodeling abilities of a cell. Triggered by their proteolytic activity cells can break down ECM components for migration or modify tissue architecture in response to biophysical or biochemical forces [97]. These changes have however important consequences on the transport and activity of autocrine and paracrine signaling molecules, both directly and indirectly [115]. Implementation of structural biomaterial remodeling in mathematical models has contributed to a better comprehension of its active role in cell signaling [120]. Translating these remodeling principles in a TE strategy has led to the development of biomaterials crosslinked by enzyme-degradable peptide sequences which

allows for a spatiotemporal control of their degradation properties [71, 100]. Models of in vivo regeneration processes (e.g. fracture healing [40]) will thereby give crucial information on the timing and location of remodeling and hence also proteolytic events. This information can be effectively implemented in treatment strategies aiming to provide continuous mechanical support to the fracture, by matching scaffold degradation with new tissue generation [105], and allows the cells to re-establish a properly working signaling environment.

In this book chapter we aim to elucidate how the key actors that govern mass transport in a TE carrier (i.e., biomaterial, cells, culture environment and solutes) can influence the overall functioning of this carrier. This will be described in terms of specific cell behavior that is provoked under defined concentrations and gradients of soluble factors. The influence of the carrier components will be captured in a series of continuum parameters that are used to formulate the mass transport problem in a mathematical landscape. Finally for each component illustrations are given on how to exploit this information in the optimization of culture conditions and the rational design of setups used for TE applications.

2 General Mass Transport in Carriers

Solute transport in biomaterial carriers (e.g., hydrogels and macro- or microporous scaffolds) used for TE applications is generally governed by passive diffusion. Diffusive transport as a primary transport mechanism in carriers can however put major constraints on the remodeling capabilities of cells that reside within this material [42] and hence also on new tissue formation. Since in this setting of dynamic tissue architecture and composition the transport of solutes with large molecular weight is most strongly affected [9], important modulations in cell signaling can be expected [120]. However also the transport of small molecules, such as oxygen, can be impeded as cells grow and new tissue is produced which gives rise to an imbalance between solute uptake and supply [25].

For this reason bioreactor systems have been developed which try to overcome fundamental limitations that are associated with diffusive mass transport. A wide variability in bioreactor configurations exists that enhance mass transport in and to the carrier, either by direct perfusion/compression or indirect perfusion/mixing [82]. Since movement and exercise are important driving forces for the body's interstitial fluid flow [120], special attention will be given here to the influence of mechanical carrier loading on solute transport.

Based on the previous discussion we introduce the general equation for mass conservation,

$$\frac{\partial C_i(x,y,z,t)}{\partial t} = -\nabla \cdot \vec{\Gamma}_i(x,y,z,t) + R_i(x,y,z,t)$$

where C_i is the concentration of the solute of interest; $\vec{\Gamma}_i$ is the mass flux; R_i is a reaction term which accounts for consumption, production, degradation, or binding of solute i to the matrix; and t is time. The mass flux due to molecular diffusion is proportional to the gradient in solute concentration ($\vec{\Gamma}_i = -D_{ij}\nabla C_i$), while convective transport is driven by the velocity field $\vec{v}$ ($\vec{\Gamma}_i = C_i\vec{v}$) [6]. Substitution of both terms into the previous equation gives (in the case of an incompressible medium),

$$\frac{\partial C_i(x,y,z,t)}{\partial t} = D_{ij}(x,y,z,t)\nabla^2 C_i(x,y,z,t) - \vec{v}(x,y,z,t)\cdot\nabla C_i(x,y,z,t) + R_i(x,y,z,t)$$

where $\vec{v}$ is the solute velocity vector; D_{ij} is the diffusion coefficient of the solute in solvent j; and ∇^2 is the Laplacian operator. This general equation applies for most biomaterial setups used in tissue engineering and its constitutive transport parameters can be determined either from experiments or from theoretical formulations.

2.1 Diffusion

Experimental quantification of solute diffusion rates through a carrier have been performed in well-controlled release kinetics experiments and by fitting analytical solutions to Fick's diffusion law [16, 25]. Also well established are fluorescence techniques to measure dispersal of fluorescently labeled target molecules, such as Fluorescence Recovery After Photobleaching (FRAP) [11], photoactivation [99], photoconversion [47] or photoswitching [3] of these fluorescent molecules. Major advantage of the latter methods is that they are less time-consuming as compared to release kinetics [11] and also have the ability to record local differences in solute diffusivity, which have been shown to result from structural matrix heterogeneities [118].

Alternatively, solute diffusion rates for a specific carrier matrix can be estimated from existing literature values. Reported values are obtained either for diffusion in free solution or for a given solute carrier combination. Based on microscale structural differences, several authors have formulated relationships which try to explain discrepancies in diffusion coefficients between often seemingly equal matrices [55, 57, 62, 95]. These models take into account the steric interactions of solutes diffusing through the matrix. The interplay between structural matrix features and effective solute diffusivity can also be described in terms of the hydrodynamic obstructions of diffusing solute. Correlations have resulted from this approach using techniques of volume averaging, which requires the use of periodic structural models [128, 129], the effective-medium approximation, which does not impose any restrictions on the structural model but is at the cost of a reduced validity and reliability of the predictions [18, 103] or by using a random walk approach [118].

2.2 Convection

Convective mass transport through a porous medium can be described using the averaged equations as formulated by Darcy or Brinkman [27]. These equations express a relation between medium velocity and the applied pressure gradient which is governed by the permeability, a factor that characterizes the influencing matrix properties. Experimental setups are described in literature that can measure different carrier permeabilities, either by applying a constant pressure or a constant flow [69, 91].

Several models are available that provide a link between structural carrier properties and permeability [49, 53]. Their application range is however constrained to approximations at the macroscopic scale since they depend on physical and geometric idealizations of the microporous carrier [120]. From the theory of mixtures and based on experimental results, it was found that the effects of induced fluid flows (which are rather low) on solute transport in the carrier are most significant for solutes with large molecular weight [35, 111].

2.3 Compression-Induced Mass Transport

Dynamic compression of a carrier combines matrix compaction with interstitial fluid transport [33]. Augmented solute transport associated with this convective fluid transport will therefore at the same time be restricted resulting from a decrease in matrix diffusivity. This compression-induced loss in diffusivity can either be measured experimentally with FRAP [38, 66] or estimated from structural diffusivity relations such as in Mackie and Meares [73, 74, 92], which assumes a high dependency of matrix diffusivity on fluid volume fraction. An interesting alternative would be the coupling of diffusive transport with structural deformation at the microscale level [117].

The effect of unconfined compression on enhanced solute transport has previously been formulated in mathematical terms using the theory of incompressible mixtures [5, 89]. In agreement with experimental observations, it was established that compression frequency and solute molecular weight are both decisive factors for the extent of compression-enhanced solute transport [32, 83]. As a major conclusion from these studies it was shown that mechanical carrier stimulation can significantly improve the transport of larger molecules (from glucose to large signaling molecules). The mechanism which underlies this phenomenon is found in the dual action of small convective flows and the increased peripheral solute gradient during dynamic loading [83].

In the next sections we will give an overview on how solute molecules with different molecular weight can influence specific cell behavior and how the transport of these molecules is influenced by the cellular carrier components. Solutes of interest range from small molecules (e.g., oxygen and glucose) to large molecules (e.g., growth factors).

3 Oxygen

The main mechanism by which cells acquire their energy is through oxidative phosphorylation [2]. In this process oxygen serves as an oxidizing agent that facilitates the flux of electrons through progressively lower energy states, which allows for a large extraction of free energy used to synthesize adenosine triphosphate (ATP) molecules. Apart from energy production, oxygen has proven to be a potent modulator of cell behavior that can change cellular phenotype [56], stimulate matrix production by the cells [94] or induce angiogenesis by the release of angiogenic factors [26]. Molecular oxygen however has a low solubility in culture medium and is rapidly consumed by the cells in order to meet their continuous energy demands. These factors make soluble oxygen very prone to become depleted during culture [42].

To what extent in time and space oxygen might become depleted within a carrier is not only regulated by the intrinsic mass transport properties of the carrier alone. A major influence comes from the cells themselves. This includes the cellular demand for dissolved oxygen, expressed by the cellular oxygen uptake rate (OUR), which is known to be controlled by many factors.

Firstly, cells harvested from distinct tissue types in the body can have significant differences in OUR [109]. Secondly, the availability of oxygen to the cells is a strong determinant of mitochondrial respiration. When cells are exposed to oxygen tensions below a critical value, the redox state of cytochrome oxidase or the respiration rate itself is partially limited [12]. This effect can be captured by a Michaelis–Menten kinetic [34],

$$Q(x,y,z,t) = Q_{\max}\frac{c_{O_2}(x,y,z,t)}{K_q + c_{O_2}(x,y,z,t)}$$

where Q is the oxygen uptake rate (mol cell^{-1} h^{-1}); Q_{max} is the maximal OUR (mol cell^{-1} h^{-1}); and K_q the oxygen tension at half of the maximal consumption rate (mol m^{-3}). Both kinetic parameters were furthermore shown to be dependent upon specific cell-material interactions [45, 80]. This relation could have important consequences related to biomaterial choice and cell remodeling behavior.

Underlying the total drop in oxygen tension inside the carrier is the effective number of metabolically active cells. Cell growth inside a biomaterial carrier can be modeled in many ways. This ranges from simple linear or piece-wise linear relationships with available nutrient concentrations [84] to more detailed models such as the modified Contois equation,

$$P_C(x,y,z,t) = c_{cell}\left[\frac{A_{cell}c^n_{O_2}(x,y,z,t)}{K_C c_{cell}\lambda\varepsilon^n_{cell} + c^n_{O_2}(x,y,z,t)} - d(x,y,z,t)\right]$$

where P_i denotes the cell growth kinetic function (cell m^{-3} day^{-1}); c_{cell} is the cell density (cell m^{-3}); A_{cell} is the homogeneous growth rate (day^{-1}); K_C is the modified Contois saturation constant; ε_{cell} is the cell volume fraction (V_{cell}/V); V_{cell}

is the averaging volume of the cell phase (m^3); V is the averaging volume (m^3); λ is a cell conversion factor (mol $cell^{-1}$); d is the death rate (day^{-1}); and n is a semi-empirical parameter. This equation inhibits cell growth in case of an overpopulation of available carrier space [19]. The Moser equation restricts cell growth in a direct relation to the available oxygen concentration [88, 104],

$$P_{Mr}(x,y,z,t) = c_{cell}\left[\frac{A_{cell}c_{O_2}^n(x,y,z,t)}{K_q\varepsilon_{cell}^n + c_{O_2}^n(x,y,z,t)} - d(x,y,z,t)\right]$$

The Moser equation reduces to the Monod equation for n equal to one. This equation couples the OUR directly to the cell growth rate as,

$$P_{Md}(x,y,z,t) = c_{cell}\left[\left(\frac{A_{cell,\max}}{Y_{CO_2}} + m_{cell}\right)\frac{c_{O_2}(x,y,z,t)}{K_q\varepsilon_{cell} + c_{O_2}(x,y,z,t)} - d(x,y,z,t)\right]$$

where $A_{cell,max}$ is the maximal specific cell growth rate (day^{-1}); Y_{CO2} is the yield of cells per unit oxygen (cells mol^{-1}); m_{cell} is the maintenance coefficient (mol $cell^{-1}$ day^{-1}), the minimum oxygen consumption required to keep the cells alive.

The main difference between linear and non-linear systems is that the former will produce a significant region of uniform proliferation, a phenomenon that is rarely observed in practice [70]. This heterogeneity can also implicitly be implemented using a custom-defined function derived from experimental data [25, 36].

Finally new matrix production and carrier remodeling can also directly alter oxygen delivery to the cells, though this effect is more pronounced for larger solutes [9, 13, 94].

In the following paragraphs we will give a brief overview on how these oxygen models can be efficiently applied to tackle some specific problems a tissue engineer could encounter. Static in vitro culture of tissue substitutes generally gives rise to heterogeneous cell growth, especially when substitute dimensions exceed a critical size [25, 80]. Enhanced proliferation of cells in the peripheral regions and coupled increases in oxygen uptake, have thereby been speculated as factors determining the incidence and severity of tissue hypoxia and associated cell death [10]. To test this hypothesis and gain improved understanding of the mechanisms which underlie these observations, mathematical models have been developed describing the interactions between oxygen tension and cell density. Effectively applying this strategy Demol et al. presented a model to describe in vitro behavior of human periosteum derived cells cultured inside a fibrin hydrogel construct (Fig. 2) [25].

Necessary model input parameters were derived from dedicated in vitro experiments that allowed to assess cell proliferation, the influence of oxygen tension on cell death and proliferation, and the diffusivity of oxygen in fibrin. As the constructs were cultivated over a period of 14 days, a significant region of dead cells in the construct center could be detected which progressively expanded outwards with longer cultivation times (Fig. 3a). The observation was accompanied by the formation of a multilayered cell sheet which had an average thickness

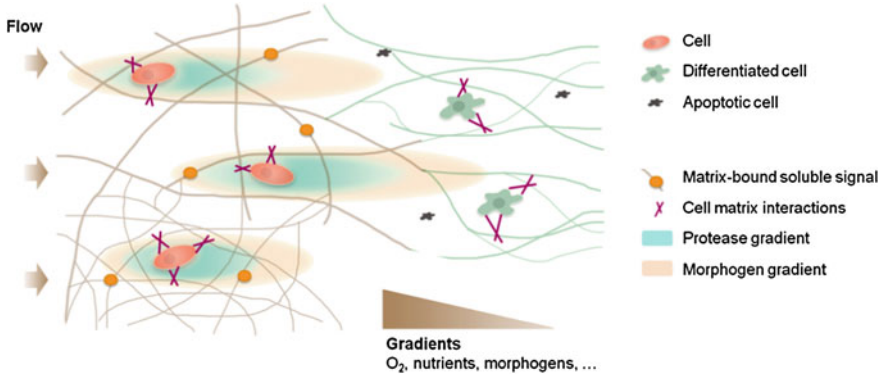

Fig. 1 Fibrous matrix remodeling is triggered by cell proteolytic activity. Transport of various solutes drives specific cell behavior during the different stages of new tissue formation (e.g., differentiation and apoptosis) and is strongly influenced by changes in carrier components (e.g., new matrix production by differentiated cells or release of matrix-bound soluble factors). Adapted from [50]

of about 40 μm and was present at the construct periphery (Fig. 3b). To account for this in the model a heterogeneous proliferation rate was implemented, with fast cell proliferation at the construct surface-its value being determined by means of a dedicated experiment-and slow proliferation inside the construct.

The model predicted the highest cell density in the outer layer (i.e., multilayered cell sheet), which was about 30 times higher than the maximum density in the rest of the gel (Fig. 4a). This led to the highest volumetric oxygen consumption rate and the highest gradient in oxygen tension in this outer layer. (Fig. 4b). However, this was not the primary cause of hypoxic regions detected within the hydrogel center, as the surface region only accounted for 2.3 % of the total decrease in oxygen tension compared to a decrease of 16.5 % in the rest of the hydrogel. This finding was further confirmed in a model parameter sensitivity analysis in which (reasonable) changes in cell sheet thickness did not have a significant influence on the occurrence of tissue hypoxia. On the contrary, variations in cellular oxygen consumption and oxygen diffusivity in the hydrogel region had a major effect on total construct hypoxia, making both governing factors for design and upscaling of static in vitro cultured hydrogel-based constructs.

As a second application we consider the development of TE pancreatic substitutes. In this field the use of mouse insulinoma βTC3 cells has since long been investigated for the long-term treatment of insulin dependent diabetes mellitus (IDDM) [28]. Reports on the insulin secretory capacities of these cells have indicated a strong reduction in secretion as the available oxygen tension drops below 10 μM [98]. This observation has therefore strong implications for the functioning of the substitute in vitro and in vivo, a problem that has been assessed using diffusion–reaction models for oxygen transport in the carrier [44]. By combining experimental measurements with the steady-state solutions of a

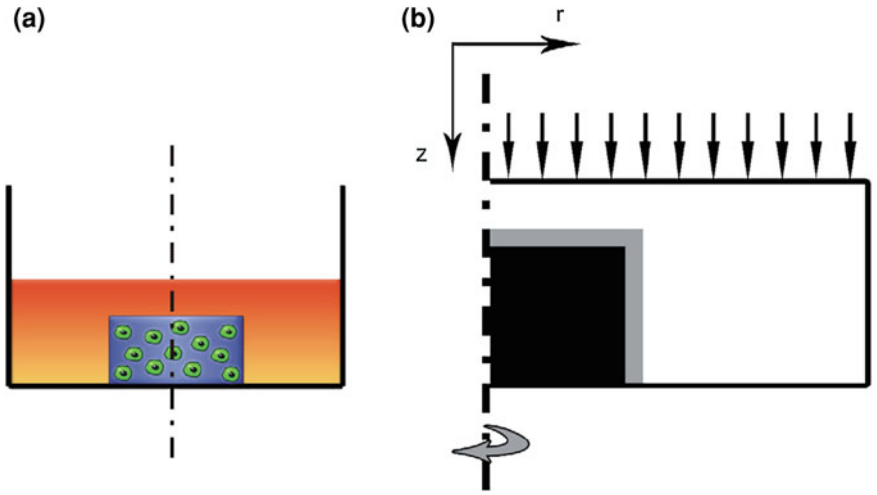

Fig. 2 **a** Schematic representation of cells cultured in a fibrin hydrogel. **b** Geometry of axisymmetric model (half of vertical cross-section) which consists of three distinct regions: cells encapsulated in the hydrogel (*black*), cells on the hydrogel surface (*grey*, not shown proportionally) and culture medium (*white*). Figure reprinted from [25]

mathematical model, these authors aimed at providing a methodology for rapid evaluation of the substitute performance. Experimental input data was obtained from ^{19}F nuclear magnetic resonance imaging on a dissolved perfluorocarbon emulsion inside the carrier. This gave a single averaged read-out of dissolved oxygen tension which showed a unique relation with the number of viable cells within the carrier, for a given environmental oxygen tension. Spatiotemporal evolution of both oxygen and viable cell density were estimated from the mathematical model using the average oxygen tension as a fitting parameter. Application of this approach therefore allowed for quick measurements on substitute functioning. Design and optimization of experimental configurations for tissue substitute cultivation and remodeling is a third important application where mathematical modeling can be of great value. Starting from this principle comparative numerical studies of bioreactor setups for in vitro tissue construct cultivation have led to an improvement of cultivation regimes and construct designs [111, 130]. These studies have indicated that reaching a critical cell mass inside the construct in vitro would require the use of a perfusion culture setup. Enhancing the transport of small molecules (such as oxygen) in perfusion systems would however require relatively high perfusion speeds. This regime demands a change in carrier geometry or biomaterial properties (e.g., stiffer matrix) in order to avoid permanent damage to the carrier. In this optimization process special attention should however be attributed to the presence of multiple soluble components, since changing the transport properties of a given solute might have important consequences for other solute transport [14, 85]. Such altered solute transport

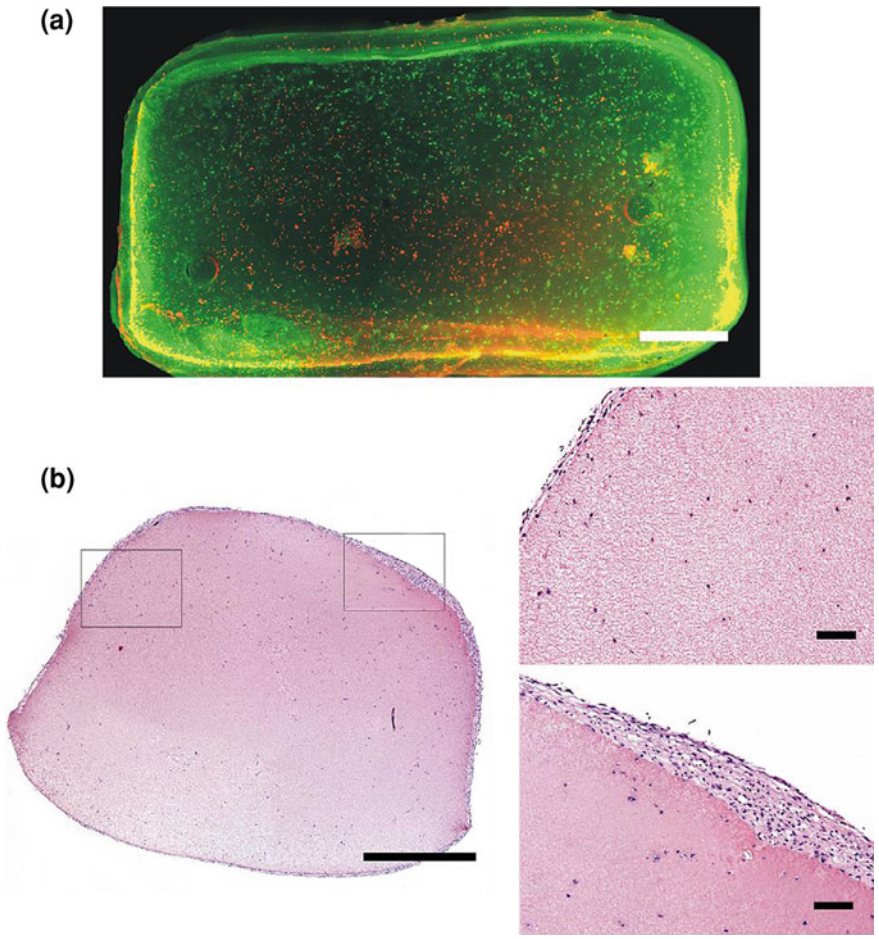

Fig. 3 **a** LIVE/DEAD viability images of human periosteum derived cells cultured for 14 days in fibrin hydrogels (bar = 1 mm). **b** H & E staining on histological sections of a fibrin construct cultured for 21 days (bar is 1 mm for the left image and 100 μm in the two images at higher magnification). Figure reprinted from [25]

could originate from differences in molecular size as described in previous sections, but could also be attributed to differences in cellular response, which will be described in the next sections.

Another strategy aiming to overcome these limitations of inadequate solute mass transport is to induce de novo synthesis of a vascular network or sprouting of existing vessels using the body as an in vivo bioreactor system [116]. The use of mathematical models has been proposed in this context as a tool for the intelligent design of scaffold structures and implantation techniques [22]. The experimental in vivo model investigated by these authors consisted of hepatocyte-seeded PLGA

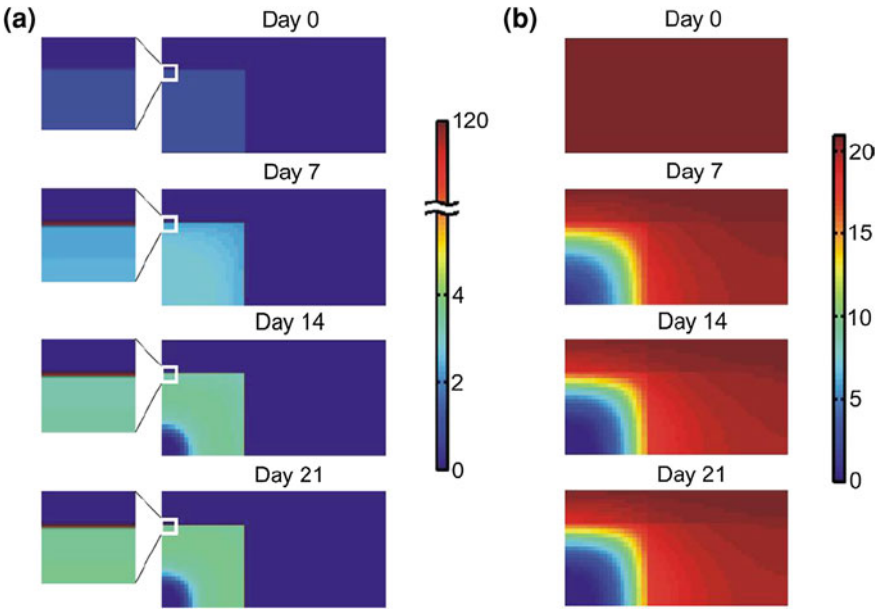

Fig. 4 Cell density (**a**) and oxygen tension (**b**) inside cell-seeded fibrin hydrogels as predicted by the mathematical model. Cell density is expressed in 10^6 cells/ml and oxygen tension in percentage. Figure reprinted from [25]

foam scaffolds with an integrated arteriovenous loop [15]. Based on the results of a computational model describing tissue growth and oxygen diffusion in the scaffold, they argued the need for a heterogeneous seeding pattern in which a small tissue biopsy of the desired tissue would be placed close to the blood vessel loop. This system would better tune angiogenesis and cell outgrowth, reducing the incidence of deficient oxygen transport to the cells and hence improve tissue functionality.

4 Nutrients and Metabolites

Cellular energy metabolism is not only dependent on the presence of a single solute, but on the entire environment of nutrients and metabolites [7, 110, 113]. Reported mechanisms of this interdependent behavior include the stimulation of OUR of cells exposed to low glucose conditions, known as the Crabtree effect [20, 51, 52, 96]. This relationship can be expressed in mathematical terms using an exponential decay function [130],

$$OUR = a_1 + a_2 e^{-c_{glc}/a_3}$$

where c_{glc} is the glucose concentration (mol m^{-3}); and a_i are parameters determined by curve fitting. A similar equation can also be applied to describe the increase in glycolysis (defined by the glucose uptake rate) for cells exposed to hypoxic conditions, known as the Pasteur effect [81, 93, 108]. In contrast to these studies other authors have reported a decrease in glycolysis under hypoxia, which would be mainly mediated by differences in medium components (e.g., presence of oxidants) [43, 67, 68, 130]. These effects should receive special attention in modeling avascular tissues, and hence also TE substitutes, since nutrient depletion could readily occur here.

It follows that solute interactions have important consequences in terms of the model predictive behavior of nutrient and metabolite gradients as well as for the optimization of experimental configurations. To illustrate this we give an example of a combined experimental and numerical study of the coupled kinetics for chondrocytes in an engineered cartilage construct [130]. In this study the relationships of oxygen and glucose uptake rates of chondrocytes exposed to different oxygen tensions, glucose concentrations and pH levels was investigated as well as the influence of lactate concentration on pH level. It was found that the predicted cell viability in the construct center was generally enhanced upon implementation of these relations in the numerical model, an observation that was most significant at high cell densities [130]. This interesting cell behavior predicted *in silico* could hence be indicative of a cellular rescue mechanism.

5 Signaling Molecules

Growth factors serve important roles as signaling molecules during development [46, 90, 119] and regeneration [17, 123]. Most of these signaling molecules need to travel through the surrounding extracellular environment either locally (autocrine signaling) or to more distant locations (paracrine and endocrine signaling) in order to exert their influence on cell behavior [112]. In the following paragraphs we will show how a cell is able to interfere with this transport process and direct this signaling reaction to provoke its intended effect. More specifically the example of cellular signaling in the growth plate will be discussed.

Bone elongation occurs through the action of endochondral ossification, which is driven primarily by the differentiation rate of proliferating chondrocytes into hypertrophic chondrocytes within the growth plate [64]. At a molecular level this process is strongly controlled by two paracrine signaling factors, Indian hedgehog (Ihh) and parathyroid hormone-related protein (PTHrP) [65, 126]. While Ihh coordinates chondrocyte proliferation, differentiation and osteoblast differentiation, PTHrP mainly keeps the proliferating chondrocytes in a proliferative phase [65, 124, 126]. Heparan sulphate (HS) complexes associated with proteoglycans in the ECM of the growth plate serve important roles in morphogenesis by providing binding sites for specific signaling molecules [8, 48]. This specificity depends on

the sulfation pattern of the heparan sulphate chains and allows for interactions with several members of the Hedgehog, transforming growth factor-β (TGFβ), bone morphogenetic protein (BMP), Wingless (Wnt/Wg), and fibroblast growth factor (FGF) families [31, 48].

Simple mathematical models have been developed expressing the total width between the early hypertrophic zone and the perichondrium using coupling equations of PTHrP and Ihh concentrations [125]. As concentrations of both signaling molecules can be modulated by various transport-related factors (e.g. mechanical compression, solute binding, changes in diffusivity due to matrix degradation) the relative importance of these factors on rates of proliferation and hypertrophy can be rapidly assessed using this model.

In a second model bone growth and morphogenesis is described by differences in spatial distribution and proliferation rates of proliferative and hypertrophied chondrocytes [37]. Underlying this growth process were the regulatory capacities of the Ihh and PTHrP spatial concentration distributions, that were modeled by a set of reaction–diffusion equations [21, 75, 78]. In order to obtain a physiological growth pattern the ratio of diffusion coefficients for both signaling molecules was bound to certain criteria. The influences of these morphogen diffusion rates on characteristics of the growth plate were acknowledged already earlier in studies of the skeletal disorder Exostosin (EXT1) [54, 63]. There it was shown that in EXT1 mutations, expressing reduced amounts of HS, the range of Ihh signaling within the growth plate was increased giving rise to an extended proliferative zone.

Calcification of the matrix surrounding the hypertrophic chondrocytes in the growth plate triggers the invasion of blood vessels from the metaphyseal bone [58]. This capillary invasion is mediated by the expression of vascular endothelial growth factor (VEGF) in hypertrophic chondrocytes [39]. Binding of VEGF to ECM components has thereby been implicated as a possible requisite for cellular autocrine signaling, giving rise to amplified VEGF gradients that are able to direct capillary morphogenesis [50, 76]. The mechanism underpinning this gradient amplification results from the combined action of a small interstitial fluid flow, biasing the secreted protease distribution, and the distribution of liberated VEGF molecules, influenced by both protease distribution and convective flows [35].

The use of growth factors (such as VEGF) in controlled-release systems has been widely proposed for TE strategies aiming at the regeneration of damaged or diseased tissues [29, 101, 102]. Given the short half-life and residence of free growth factors in solution, controlled-release strategies hold great promise providing a means to protect these factors from degradation and internalization [77, 105]. Though such systems can deliver signaling molecules in a time- and space-controlled manner, the lack of detailed knowledge on in vivo growth factor concentrations and possible interfering behavior of administered compounds complicates rational decisions on the required growth factor concentrations [60]. For such applications we can however greatly take advantage of the use of numerical models. In this way a modeling-based design approach was proposed for the controlled delivery of VEGF in a mouse model of hindlimb ischemia [16]. Using a reaction diffusion model to predict VEGF distribution in vivo, a layered scaffold

design was proposed to deliver VEGF in a spatial concentration gradient where it is able to both initiate and spatially control angiogenesis. Regulating spatial VEGF presentation increased hindlimb blood flow which was reflected in a reduced incidence of limb necrosis.

Other more detailed numerical models of in vivo regeneration processes could equally well be applied for the rational design of controlled delivery systems [40]. Such models have the added advantage of testing the efficacy of a certain treatment strategy (such as controlled-delivery systems) *in silico*, hence helping researchers to identify the most promising strategies and having the potential to significantly reduce experimental costs [41].

6 Discussion and Conclusions

Proper functionalizaton of carriers used for TE applications, requires a profound understanding of the mechanisms that drive solute transport to and from the active cell units. These solutes can be as small as oxygen, essential for cellular nutrition, or as large as protein complexes, which allow cells to communicate with each other or probe their environment [122]. The cellular actions they can elicit range from basic cell survival and division to the organized patterning of cells into tissues (i.e., morphogenesis).

Mimicking the normal in vivo solute transport environment of a cell and optimization of culture conditions is complicated by the various mechanisms which underlie these transport processes. We have shown that this variability can be induced by differences in molecular size between solutes, differences in synthesis and uptake of solutes by the cell, interactions at a cell level between various nutrients and metabolites (but also signaling molecules [4, 106]), solute interactions with the surrounding matrix and many others. Systems that involve such high degrees of complexity can however greatly benefit from mathematical modeling, as we have shown in this chapter.

Choosing an optimal model and setting an appropriate level of detail is strongly determined by the extent of construct remodeling that is taking place, the availability and type of experimental data, and spatial resolution [107]. Focus in this chapter has been mainly set on single scale (continuum) models which is ascribed to their abundant availability and their low computational costs. If we however want to recreate interactions at multiple levels of organization with respect to space and time, more attention should be attributed to the integrative properties of the model [114], a strategy that has been defined in literature as multiscale modeling. Crucial to the success of a multiscale modeling framework, is to provide a consistent cross-scale linkage interface between the models at each biological level [23]. We have shown the importance of such an interface in the context of diffusive transport within TE carriers, by providing a means to correlate microstructural matrix properties to solute diffusion rates using for example a volume averaging technique [129].

Finally it should be mentioned that diffusion–reaction mechanisms are not only prominent for solute transport inside the carrier, also inside a cell these mechanisms are important for proper cell functioning (for example in signal propagation [59]). Information generation by the use of solute gradients is accordingly a widely conserved mechanism in biology, operating at multiple scales of organization [87]. This scale-invariant principle holds great promise by extending the applicability of both models and imaging techniques that were described within this chapter.

References

1. Acosta, M.A., Ymele-Leki, P., Kostov, Y.V., Leach, J.B.: Fluorescent microparticles for sensing cell microenvironment oxygen levels within 3D scaffolds. Biomaterials **30**(17), 3068–3074 (2009). doi:10.1016/j.biomaterials.2009.02.021
2. Alberts, B., Johnson, A., Lewis, J., Raff, M., Roberts, K., Walter, P.: Molecular Biology of the Cell, 4th edn. Garland Science, New York (2007)
3. Ando, R., Mizuno, H., Miyawaki, A.: Regulated fast nucleocytoplasmic shuttling observed by reversible protein highlighting. Science **306**(5700), 1370–1373 (2004). doi:10.1126/science.1102506. 306/5700/1370[pii]
4. Arany, Z., Foo, S.Y., Ma, Y.H., Ruas, J.L., Bommi-Reddy, A., Girnun, G., Cooper, M., Laznik, D., Chinsomboon, J., Rangwala, S.M., Baek, K.H., Rosenzweig, A., Spiegelman, B.M.: HIF-independent regulation of VEGF and angiogenesis by the transcriptional coactivator PGC-1 alpha. Nature **451**(7181), 1008–U1008 (2008). doi:10.1038/Nature06613
5. Armstrong, C.G., Lai, W.M., Mow, V.C.: An analysis of the unconfined compression of articular-cartilage. J. Biomech. Eng. Trans. ASME **106**(2), 165–173 (1984)
6. Beard, D.A., Qian, H.: Chemical Biophysics: Quantitative Analysis of Cellular Systems. Cambridge Texts in Biomedical Engineering. Cambridge University Press, New York (2008)
7. Bibby, S.R.S., Jones, D.A., Ripley, R.M., Urban, J.P.G.: Metabolism of the intervertebral disc: effects of low levels of oxygen, glucose, and pH on rates of energy metabolism of bovine nucleus pulposus cells. Spine **30**(5), 487–496 (2005)
8. Bishop, J.R., Schuksz, M., Esko, J.D.: Heparan sulphate proteoglycans fine-tune mammalian physiology. Nature **446**(7139), 1030–1037 (2007). doi:10.1038/Nature05817
9. Blum, J.J., Lawler, G., Reed, M., Shin, I.: Effect of cytoskeletal geometry on intracellular diffusion. Biophys. J. **56**(5), 995–1005 (1989). doi:10.1016/S0006-3495(89)82744-4. S0006-3495(89)82744-4[pii]
10. Brown, D.A., MacLellan, W.R., Laks, H., Dunn, J.C., Wu, B.M., Beygui, R.E.: Analysis of oxygen transport in a diffusion-limited model of engineered heart tissue. Biotechnol. Bioeng. **97**(4), 962–975 (2007). doi:10.1002/bit.21295
11. Brown, E.B., Wu, E.S., Zipfel, W., Webb, W.W.: Measurement of molecular diffusion in solution by multiphoton fluorescence photobleaching recovery. Biophys. J. **77**(5), 2837–2849 (1999)
12. Brown, G.C.: Control of respiration and Atp synthesis in mammalian mitochondria and cells. Biochem. J. **284**, 1–13 (1992)
13. Bursac, P.M., Freed, L.E., Biron, R.J., Vunjak-Novakovic, G.: Mass transfer studies of tissue engineered cartilage. Tissue Eng. **2**(2), 141–150 (1996). doi:10.1089/ten.1996.2.141
14. Cartmell, S.H., Porter, B.D., Garcia, A.J., Guldberg, R.E.: Effects of medium perfusion rate on cell-seeded three-dimensional bone constructs in vitro. Tissue Eng. **9**(6), 1197–1203 (2003)
15. Cassell, O.C., Morrison, W.A., Messina, A., Penington, A.J., Thompson, E.W., Stevens, G.W., Perera, J.M., Kleinman, H.K., Hurley, J.V., Romeo, R., Knight, K.R.: The influence of extracellular matrix on the generation of vascularized, engineered, transplantable tissue. Ann. N. Y. Acad. Sci. **944**, 429–442 (2001)

16. Chen, R.R., Silva, E.A., Yuen, W.W., Brock, A.A., Fischbach, C., Lin, A.S., Guldberg, R.E., Mooney, D.J.: Integrated approach to designing growth factor delivery systems. FASEB J. **21**(14), 3896–3903 (2007). doi:10.1096/fj.06-7873com
17. Chen, Y., Whetstone, H.C., Lin, A.C., Nadesan, P., Wei, Q.X., Poon, R., Alman, B.A.: Beta-catenin signaling plays a disparate role in different phases of fracture repair: implications for therapy to improve bone healing. PLoS Med **4**(7), 1216–1229 (2007). doi:10.1371/journal.pmed.0040249. ARTN e249
18. Clague, D.S., Phillips, R.J.: Hindered diffusion of spherical macromolecules through dilute fibrous media. Phys. Fluids **8**(7), 1720–1731 (1996)
19. Contois, D.E.: Kinetics of bacterial growth: relationship between population density and specific growth rate of continuous cultures. J. Gen. Microbiol. **21**, 40–50 (1959)
20. Crabtree, H.G.: Observations on the carbohydrate metabolism of tumours. Biochem. J. **23**(3), 536–545 (1929)
21. Crampin, E.J., Hackborn, W.W., Maini, P.K.: Pattern formation in reaction-diffusion models with nonuniform domain growth. Bull. Math. Biol. **64**(4), 747–769 (2002). doi:10.1006/bulm.2002.0295
22. Croll, T.I., Gentz, S., Mueller, K., Davidson, M., O'Connor, A.J., Stevens, G.W., Cooper-White, J.J.: Modelling oxygen diffusion and cell growth in a porous, vascularising scaffold for soft tissue engineering applications. Chem. Eng. Sci. **60**(17), 4924–4934 (2005). doi:10.1016/j.cea.2005.03.051
23. Dallon, J.C.: Multiscale modeling of cellular systems in biology. Curr. Opin. Colloid Interface Sci. **15**(1–2), 24–31 (2010). doi:10.1016/j.cocis.2009.05.007
24. Dehmelt, L., Bastiaens, P.I.H.: Spatial organization of intracellular communication: insights from imaging. Nat. Rev. Mol. Cell Biol. **11**(6), 440–452 (2010). doi:10.1038/Nrm2903
25. Demol, J., Lambrechts, D., Geris, L., Schrooten, J., Van Oosterwyck, H.: Towards a quantitative understanding of oxygen tension and cell density evolution in fibrin hydrogels. Biomaterials **32**(1), 107–118 (2011). doi:10.1016/j.biomaterials.2010.08.093
26. Dor, Y., Porat, R., Keshet, E.: Vascular endothelial growth factor and vascular adjustments to perturbations in oxygen homeostasis. Am. J. Physiol. Cell Physiol. **280**(6), C1367–C1374 (2001)
27. Durlofsky, L., Brady, J.F.: Analysis of the Brinkman equation as a model for flow in porous-media. Phys. Fluids **30**(11), 3329–3341 (1987)
28. Efrat, S., Linde, S., Kofod, H., Spector, D., Delannoy, M., Grant, S., Hanahan, D., Baekkeskov, S.: Beta-cell lines derived from transgenic mice expressing a hybrid insulin gene-oncogene. Proc. Natl. Acad. Sci. U. S. A. **85**(23), 9037–9041 (1988)
29. Elisseeff, J., McIntosh, W., Fu, K., Blunk, T., Langer, R.: Controlled-release of IGF-I and TGF-beta 1 in a photopolymerizing hydrogel for cartilage tissue engineering. J. Orthop. Res. **19**(6), 1098–1104 (2001)
30. Engler, A.J., Sen, S., Sweeney, H.L., Discher, D.E.: Matrix elasticity directs stem cell lineage specification. Cell **126**(4), 677–689 (2006). doi:10.1016/j.cell.2006.06.044. S0092-8674(06)00961-5[pii]
31. Esko, J.D., Selleck, S.B.: Order out of chaos: assembly of ligand binding sites in heparan sulfate. Annu. Rev. Biochem. **71**, 435–471 (2002). doi:10.1146/annurev.biochem.71.110601.13545
32. Evans, R.C., Quinn, T.M.: Dynamic compression augments interstitial transport of a glucose-like solute in articular cartilage. Biophys. J. **91**(4), 1541–1547 (2006). doi:10.1529/biophysj.105.080366
33. Evans, R.C., Quinn, T.M.: Solute convection in dynamically compressed cartilage. J. Biomech. **39**(6), 1048–1055 (2006). doi:10.1016/j.jbiomech.2005.02.017. S0021-9290(05)00127-2[pii]
34. Fassnacht, D., Portner, R.: Experimental and theoretical considerations on oxygen supply for animal cell growth in fixed-bed reactors. J. Biotechnol. **72**(3), 169–184 (1999). S0168165699001297[pii]
35. Fleury, M.E., Boardman, K.C., Swartz, M.A.: Autologous morphogen gradients by subtle interstitial flow and matrix interactions. Biophys. J. **91**(1), 113–121 (2006). doi:10.1529/biophysj.105.080192

36. Galban, C.J., Locke, B.R.: Analysis of cell growth kinetics and substrate diffusion in a polymer scaffold. Biotechnol. Bioeng. **65**(2), 121–132 (1999)
37. Garzon-Alvarado, D.A., Garcia-Aznar, J.M., Doblare, M.: A reaction-diffusion model for long bones growth. Biomech. Model. Mechan. **8**(5), 381–395 (2009). doi:10.1007/s10237-008-0144-z
38. Gefen, A., Cornelissen, L.H., Gawlitta, D., Bader, D.L., Oomens, C.W.: The free diffusion of macromolecules in tissue-engineered skeletal muscle subjected to large compression strains. J. Biomech. **41**(4), 845–853 (2008). doi:10.1016/j.jbiomech.2007.10.023. S0021-9290(07)00471-X[pii]
39. Gerber, H.P., Vu, T.H., Ryan, A.M., Kowalski, J., Werb, Z., Ferrara, N.: VEGF couples hypertrophic cartilage remodeling, ossification and angiogenesis during endochondral bone formation. Nat. Med. **5**(6), 623–628 (1999)
40. Geris, L., Gerisch, A., Maes, C., Carmeliet, G., Weiner, R., Vander Sloten, J., Van Oosterwyck, H.: Mathematical modeling of fracture healing in mice: comparison between experimental data and numerical simulation results. Med. Biol. Eng. Comput. **44**(4), 280–289 (2006). doi:10.1007/s11517-006-0040-6
41. Geris, L., Schugart, R., Van Oosterwyck, H.: In silico design of treatment strategies in wound healing and bone fracture healing. Philos. Trans. A Math. Phys. Eng. Sci. **368**(1920), 2683–2706 (2010). doi:10.1098/rsta.2010.0056. 368/1920/2683[pii]
42. Griffith, L.G., Swartz, M.A.: Capturing complex 3D tissue physiology in vitro. Nat. Rev. Mol. Cell Biol. **7**(3), 211–224 (2006). doi:10.1038/Nrm1858
43. Grimshaw, M.J., Mason, R.M.: Bovine articular chondrocyte function in vitro depends upon oxygen tension. Osteoarthr. Cartil. **8**(5), 386–392 (2000). doi:10.1053/joca.1999.0314. S1063-4584(99)90314-X[pii]
44. Gross, J.D., Constantinidis, I., Sambanis, A.: Modeling of encapsulated cell systems. J. Theor. Biol. **244**(3), 500–510 (2007). doi:10.1016/j.jtbi.2006.08.012. S0022-5193(06)00365-1[pii]
45. Guaccio, A., Borselli, C., Oliviero, O., Netti, P.A.: Oxygen consumption of chondrocytes in agarose and collagen gels: a comparative analysis. Biomaterials **29**(10), 1484–1493 (2008). doi:10.1016/j.biomaterials.2007.12.020
46. Gurdon, J.B., Bourillot, P.Y.: Morphogen gradient interpretation. Nature **413**(6858), 797–803 (2001)
47. Gurskaya, N.G., Verkhusha, V.V., Shcheglov, A.S., Staroverov, D.B., Chepurnykh, T.V., Fradkov, A.F., Lukyanov, S., Lukyanov, K.A.: Engineering of a monomeric green-to-red photoactivatable fluorescent protein induced by blue light. Nat. Biotechnol. **24**(4), 461–465 (2006). doi:10.1038/Nbt1191
48. Hacker, U., Nybakken, K., Perrimon, N.: Heparan sulphate proteoglycans: the sweet side of development. Nat. Rev. Mol. Cell Biol. **6**(7), 530–541 (2005). 10.1038/nrm1681]nrm1681[pii]
49. Happel, J.: Viscous flow relative to arrays of cylinders. AIChE J. **5**(2), 174–177 (1959)
50. Helm, C.L.E., Fleury, M.E., Zisch, A.H., Boschetti, F., Swartz, M.A.: Synergy between interstitial flow and VEGF directs capillary morphogenesis in vitro through a gradient amplification mechanism. Proc. Natl. Acad. Sci. U. S. A. **102**(44), 15779–15784 (2005). doi:10.1073/pnas.0503681102
51. Heywood, H.K., Bader, D.L., Lee, D.A.: Rate of oxygen consumption by isolated articular chondrocytes is sensitive to medium glucose concentration. J. Cell. Physiol. **206**(2), 402–410 (2006). doi:10.1002/Jcp.20491
52. Heywood, H.K., Knight, M.M., Lee, D.A.: Both superficial and deep zone articular chondrocyte subpopulations exhibit the crabtree effect but have different basal oxygen consumption rates. J. Cell. Physiol. **223**(3), 630–639 (2010). doi:10.1002/Jcp.22061
53. Higdon, J.J.L., Ford, G.D.: Permeability of three-dimensional models of fibrous porous media. J. Fluid Mech. **308**, 341–361 (1996)
54. Hilton, M.J., Gutierrez, L., Martinez, D.A., Wells, D.E.: EXT1 regulates chondrocyte proliferation and differentiation during endochondral bone development. Bone **36**(3), 379–386 (2005). doi:10.1016/j.bone.2004.09.025

55. Hrabe, J., Hrabetova, S., Segeth, K.: A model of effective diffusion and tortuosity in the extracellular space of the brain. Biophys. J. **87**(3), 1606–1617 (2004). doi:10.1529/biophysj.103.039495
56. Hunziker, E.B., Driesang, I.M.: Functional barrier principle for growth-factor-based articular cartilage repair. Osteoarthr. Cartil. **11**(5), 320–327 (2003). S1063458403000311[pii]
57. Johansson, L., Lofroth, J.E.: Diffusion and interaction in gels and solutions. 4. Hard-sphere Brownian dynamics simulations. J. Chem. Phys. **98**(9), 7471–7479 (1993)
58. Karsenty, G., Wagner, E.F.: Reaching a genetic and molecular understanding of skeletal development. Dev. Cell **2**(4), 389–406 (2002)
59. Kholodenko, B.N.: Cell-signalling dynamics in time and space. Nat. Rev. Mol. Cell Biol. **7**(3), 165–176 (2006). doi:10.1038/Nrm1838
60. Kirkpatrick, C.J., Fuchs, S., Unger, R.E.: Co-culture systems for vascularization—learning from nature. Adv. Drug Deliv. Rev. **63**(4–5), 291–299 (2011). doi:10.1016/j.addr.2011.01.009
61. Kleinman, H.K., Philp, D., Hoffman, M.P.: Role of the extracellular matrix in morphogenesis. Curr. Opin. Biotechnol. **14**(5), 526–532 (2003). S0958166903001186[pii]
62. Kosto, K.B., Deen, W.M.: Diffusivities of macromolecules in composite hydrogels. AIChE J. **50**(11), 2648–2658 (2004). doi:10.1002/Aic.10216
63. Koziel, L., Kunath, M., Kelly, O.G., Vortkamp, A.: Ext1-dependent heparan sulfate regulates the range of Ihh signaling during endochondral ossification. Dev. Cell **6**(6), 801–813 (2004)
64. Kronenberg, H.M.: Developmental regulation of the growth plate. Nature **423**(6937), 332–336 (2003). doi:10.1038/Nature01657
65. Lanske, B., Karaplis, A.C., Lee, K., Luz, A., Vortkamp, A., Pirro, A., Karperien, M., Defize, L.H.K., Ho, C., Mulligan, R.C., AbouSamra, A.B., Juppner, H., Segre, G.V., Kronenberg, H.M.: PTH/PTHrP receptor in early development and Indian hedgehog-regulated bone growth. Science **273**(5275), 663–666 (1996)
66. Leddy, H.A., Guilak, F.: Site-specific effects of compression on macromolecular diffusion in articular cartilage. Biophys. J. **95**(10), 4890–4895 (2008). doi:10.1529/biophysj.108.137752
67. Lee, R.B., Urban, J.P.: Evidence for a negative Pasteur effect in articular cartilage. Biochem. J. **321**(Pt 1), 95–102 (1997)
68. Lee, R.B., Urban, J.P.: Functional replacement of oxygen by other oxidants in articular cartilage. Arthritis Rheum. **46**(12), 3190–3200 (2002). doi:10.1002/art.10686
69. Levick, J.R.: Flow through interstitium and other fibrous matrices. Q. J. Exp. Physiol. CMS **72**(4), 409–438 (1987)
70. Lewis, M.C., MacArthur, B.D., Malda, J., Pettet, G., Please, C.P.: Heterogeneous proliferation within engineered cartilaginous tissue: the role of oxygen tension. Biotechnol. Bioeng. **91**(5), 607–615 (2005). doi:10.1002/Bit.20508
71. Lutolf, M.P., Hubbell, J.A.: Synthetic biomaterials as instructive extracellular microenvironments for morphogenesis in tissue engineering. Nat. Biotechnol. **23**(1), 47–55 (2005). doi:10.1038/Nbt1055
72. Lutolf, M.R., Weber, F.E., Schmoekel, H.G., Schense, J.C., Kohler, T., Muller, R., Hubbell, J.A.: Repair of bone defects using synthetic mimetics of collagenous extracellular matrices. Nat. Biotechnol. **21**(5), 513–518 (2003). doi:10.1038/Nbt818
73. Mackie, J.S., Meares, P.: The diffusion of electrolytes in a cation-exchange resin membrane. 1. Theoretical. Proc. R. Soc. Lond. Ser. A **232**(1191), 498–509 (1955a)
74. Mackie, J.S., Meares, P.: The diffusion of electrolytes in a cation-exchange resin membrane. 2. Experimental. Proc. R. Soc. Lond. Ser. A **232**(1191), 510–518 (1955b)
75. Madzvamuse, A.: Time-stepping schemes for moving grid finite elements applied to reaction-diffusion systems on fixed and growing domains. J. Comput. Phys. **214**(1), 239–263 (2006). doi:10.1016/j.jcp.2005.09.012
76. Maes, C., Carmeliet, G.: Vascular and nonvascular roles of VEGF in bone development. In: Ruhrberg, C. (ed.) VEGF in Development, pp. 79–90. Springer, New York (2008)
77. Mahoney, M.J., Krewson, C., Miller, J., Saltzman, W.M.: Impact of cell type and density on nerve growth factor distribution and bioactivity in 3-dimensional collagen gel cultures. Tissue Eng. **12**(7), 1915–1927 (2006)

78. Maini, P.K.: Using mathematical models to help understand biological pattern formation. C. R. Biol. **327**(3), 225–234 (2004). doi:10.1016/j.crvi.2003.05.006
79. Makarenkova, H.P., Hoffman, M.P., Beenken, A., Eliseenkova, A.V., Meech, R., Tsau, C., Patel, V.N., Lang, R.A., Mohammadi, M.: Differential interactions of FGFs with heparan sulfate control gradient formation and branching morphogenesis. Sci. Signal **2**(88), ra55 (2009). doi:2/88/ra55[pii]10.1126/scisignal.2000304
80. Malda, J., Rouwkema, J., Martens, D.E., le Comte, E.P., Kooy, F.K., Tramper, J., van Blitterswijk, C.A., Riesle, J.: Oxygen gradients in tissue-engineered PEGT/PBT cartilaginous constructs: measurement and modeling. Biotechnol. Bioeng. **86**(1), 9–18 (2004). doi:10.1002/Bit.20038
81. Marcus, R.E.: The effect of low oxygen concentration on growth, glycolysis, and sulfate incorporation by articular chondrocytes in monolayer culture. Arthritis Rheum. **16**(5), 646–656 (1973)
82. Martin, I., Wendt, D., Heberer, M.: The role of bioreactors in tissue engineering. Trends Biotechnol. **22**(2), 80–86 (2004). doi:10.1016/j.tibtech.2003.12.001
83. Mauck, R.L., Hung, C.T., Ateshian, G.A.: Modeling of neutral solute transport in a dynamically loaded porous permeable gel: Implications for articular cartilage biosynthesis and tissue engineering (vol. 125, 602, 2003). J. Biomech. Eng. Trans. ASME **126**(3), 392–392 (2004)
84. Mcelwain, D.L.S., Ponzo, P.J.: Model for growth of a solid tumor with nonuniform oxygen-consumption. Math. Biosci. **35**(3–4), 267–279 (1977)
85. Mizuno, S., Allemann, F., Glowacki, J.: Effects of medium perfusion on matrix production by bovine chondrocytes in three-dimensional collagen sponges. J. Biomed. Mater. Res. **56**(3), 368–375 (2001). doi:10.1002/1097-4636(20010905). 56:3<368:AID-JBM1105>3.0.CO;2-V[pii]
86. Mizutani, C.M., Nie, Q., Wan, F.Y.M., Zhang, Y.T., Vilmos, P., Sousa-Neves, R., Bier, E., Marsh, J.L., Lander, A.D.: Formation of the BMP activity gradient in the Drosophila embryo. Dev. Cell **8**(6), 915–924 (2005). doi:10.1016/j.devcel.2005.04.009
87. Moseley, J.B., Mayeux, A., Paoletti, A., Nurse, P.: A spatial gradient coordinates cell size and mitotic entry in fission yeast. Nature **459**(7248), 857–U858 (2009). doi:10.1038/Nature08074
88. Moser, H.: Structure and dynamics of bacterial populations maintained in the chemostat. Cold Spring Harb. Symp. Quant. Biol. **22**, 121–137 (1957)
89. Mow, V.C., Kuei, S.C., Lai, W.M., Armstrong, C.G.: Biphasic creep and stress relaxation of articular cartilage in compression? Theory and experiments. J. Biomech. Eng. **102**(1), 73–84 (1980)
90. Murry, C.E., Keller, G.: Differentiation of embryonic stem cells to clinically relevant populations: lessons from embryonic development. Cell **132**(4), 661–680 (2008). doi:10.1016/j.cell.2008.02.008
91. Ng, C.P., Swartz, M.A.: Fibroblast alignment under interstitial fluid flow using a novel 3-D tissue culture model. Am. J. Physiol. Heart Circ. Physiol. **284**(5), H1771–H1777 (2003). doi:10.1152/ajpheart.01008.2002
92. Nimer, E., Schneiderman, R., Maroudas, A.: Diffusion and partition of solutes in cartilage under static load. Biophys. Chem. **106**(2), 125–146 (2003). doi:10.1016/S0301-4622(03)00157-1
93. Obradovic, B., Carrier, R.L., Vunjak-Novakovic, G., Freed, L.E.: Gas exchange is essential for bioreactor cultivation of tissue engineered cartilage. Biotechnol. Bioeng. **63**(2), 197–205 (1999). doi:10.1002/(SICI)1097-0290(19990420). 63:2<197:AID-BIT8>3.0.CO;2-2[pii]
94. Obradovic, B., Meldon, J.H., Freed, L.E., Vunjak-Novakovic, G.: Glycosaminoglycan deposition in engineered cartilage: experiments and mathematical model. AIChE J. **46**(9), 1860–1871 (2000)
95. Ogston, A.G., Preston, B.N., Wells, J.D., Ogston, A.G., Preston, B.N., Snowden, J.M., Wells, J.D.: Transport of compact particles through solutions of chain-polymers. Proc. R. Soc. Lond. A Mat. **333**(1594), 297–316 (1973)
96. Otte, P.: Basic cell metabolism of articular cartilage. Manometric studies. Z. Rheumatol. **50**(5), 304–312 (1991)

97. Page-McCaw, A., Ewald, A.J., Werb, Z.: Matrix metalloproteinases and the regulation of tissue remodelling. Nat. Rev. Mol. Cell Biol. **8**(3), 221–233 (2007). doi:10.1038/nrm2125. nrm2125 [pii]
98. Papas, K.K., Long Jr, R.C., Constantinidis, I., Sambanis, A.: Effects of oxygen on metabolic and secretory activities of beta TC3 cells. Biochim. Biophys. Acta **1291**(2), 163–166 (1996). 0304-4165(96)00062-1[pii]
99. Patterson, G.H., Lippincott-Schwartz, J.: A photoactivatable GFP for selective photolabeling of proteins and cells. Science **297**(5588), 1873–1877 (2002)
100. Patterson, J., Martino, M.M., Hubbell, J.A.: Biomimetic materials in tissue engineering. Mater. Today **13**(1–2), 14–22 (2010)
101. Phelps, E.A., Landazuri, N., Thule, P.M., Taylor, W.R., Garcia, A.J.: Bioartificial matrices for therapeutic vascularization. Proc. Natl. Acad. Sci. U. S. A. **107**(8), 3323–3328 (2010). doi:10.1073/pnas.0905447107
102. Phillips, J.E., Burns, K.L., Le Doux, J.M., Guldberg, R.E., Garcia, A.J.: Engineering graded tissue interfaces. Proc. Natl. Acad. Sci. U. S. A. **105**(34), 12170–12175 (2008). doi:10.1073/pnas.0801988105. 0801988105 [pii]
103. Phillips, R.J., Deen, W.M., Brady, J.F.: Hindered transport of spherical macromolecules in fibrous membranes and gels. AIChE J. **35**(11), 1761–1769 (1989)
104. Picioreanu, C., van Loosdrecht, M.C., Heijnen, J.J.: A new combined differential-discrete cellular automaton approach for biofilm modeling: application for growth in gel beads. Biotechnol. Bioeng. **57**(6), 718–731 (1998). doi:10.1002/(SICI)1097-0290(19980320)57:6<718:AID-BIT9>. 3.0.CO;2-O [pii]
105. Place, E.S., Evans, N.D., Stevens, M.M.: Complexity in biomaterials for tissue engineering. Nat. Mater. **8**(6), 457–470 (2009). doi:10.1038/Nmat2441
106. Pugh, C.W., Ratcliffe, P.J.: Regulation of angiogenesis by hypoxia: role of the HIF system. Na.t Med. **9**(6), 677–684 (2003). doi:10.1038/nm0603-677nm0603-677 [pii]
107. Qutub, A.A., Mac Gabhann, F., Karagiannis, E.D., Vempati, P., Popel, A.S.: Multiscale models of angiogenesis. IEEE Eng. Med. Biol. Mag. **28**(2), 14–31 (2009). doi:10.1109/MEMB.2009.931791
108. Rajpurohit, R., Koch, C.J., Tao, Z., Teixeira, C.M., Shapiro, I.M.: Adaptation of chondrocytes to low oxygen tension: relationship between hypoxia and cellular metabolism. J. Cell. Physiol. **168**(2), 424–432 (1996). doi:10.1002/(SICI)1097-4652(199608). 168:2<424:AID-JCP21>3.0.CO;2-1[pii]10.1002/(SICI)1097-4652(199608)168:2<424:AID-JCP21>3.0.CO;2-1
109. Rolfe, D.F., Brown, G.C.: Cellular energy utilization and molecular origin of standard metabolic rate in mammals. Physiol. Rev. **77**(3), 731–758 (1997)
110. Sengers, B.G., Heywood, H.K., Lee, D.A., Oomens, C.W.J., Bader, D.L.: Nutrient utilization by bovine articular chondrocytes: A combined experimental and theoretical approach. J. Biomech. Eng. Trans. ASME **127**(5), 758–766 (2005). doi:10.1115/1.1993664
111. Sengers, B.G., van Donkelaar, C.C., Oomens, C.W.J., Baaijens, F.P.T.: Computational study of culture conditions and nutrient supply in cartilage tissue engineering. Biotechnol. Prog. **21**(4), 1252–1261 (2005). doi:10.1021/Bp0500157
112. Singh, A.B., Harris, R.C.: Autocrine, paracrine and juxtacrine signaling by EGFR ligands. Cell. Signal. **17**(10), 1183–1193 (2005). doi:10.1016/j.cellsig.2005.03.026
113. Soukane, D.M., Shirazi-Adl, A., Urban, J.P.G.: Computation of coupled diffusion of oxygen, glucose and lactic acid in an intervertebral disc. J. Biomech. **40**(12), 2645–2654 (2007). doi:10.1016/j.jbiomech.2007.01.003
114. Southern, J., Pitt-Francis, J., Whiteley, J., Stokeley, D., Kobashi, H., Nobes, R., Kadooka, Y., Gavaghan, D.: Multi-scale computational modelling in biology and physiology. Prog. Biophys. Mol. Biol. **96**(1–3), 60–89 (2008). doi:10.1016/j.pbiomolbio.2007.07.019. S0079-6107(07)00067-3 [pii]
115. Sternlicht, M.D., Werb, Z.: How matrix metalloproteinases regulate cell behavior. Annu. Rev. Cell Dev. Biol. **17**, 463–516 (2001)

116. Stevens, M.M., Marini, R.P., Schaefer, D., Aronson, J., Langer, R., Shastri, V.P.: In vivo engineering of organs: the bone bioreactor. Proc. Natl. Acad. Sci. U. S. A. **102**(32), 11450–11455 (2005). doi:10.1073/pnas.0504705102. 0504705102 [pii]
117. Stylianopoulos, T., Barocas, V.H.: Volume-averaging theory for the study of the mechanics of collagen networks. Comput. Method Appl. Mech. Eng. **196**(31–32), 2981–2990 (2007). doi:10.1016/j.cma.2006.06.019
118. Stylianopoulos, T., Diop-Frimpong, B., Munn, L.L., Jain, R.K.: Diffusion anisotropy in collagen gels and tumors: the Effect of fiber network orientation. Biophys. J. **99**(10), 3119–3128 (2010). doi:10.1016/j.bpj.2010.08.065
119. Sumi, T., Tsuneyoshi, N., Nakatsuji, N., Suemori, H.: Defining early lineage specification of human embryonic stem cells by the orchestrated balance of canonical Wnt/beta-catenin. Activin/Nodal BMP signal. Dev. **135**(17), 2969–2979 (2008). doi:10.1242/Dev.021121
120. Swartz, M.A., Fleury, M.E.: Interstitial flow and its effects in soft tissues. Annu. Rev. Biomed. Eng. **9**, 229–256 (2007). doi:10.1146/annure/bioeng.9.060906.151850
121. Teleman, A.A., Strigini, M., Cohen, S.M.: Shaping morphogen gradients. Cell **105**(5), 559–562 (2001). S0092-8674(01)00377-4 [pii]
122. Tschumperlin, D.J., Dai, G.H., Maly, I.V., Kikuchi, T., Laiho, L.H., McVittie, A.K., Haley, K.J., Lilly, C.M., So, P.T.C., Lauffenburger, D.A., Kamm, R.D., Drazen, J.M.: Mechanotransduction through growth-factor shedding into the extracellular space. Nature **429**(6987), 83–86 (2004)
123. Tsuji, K., Bandyopadhyay, A., Harfe, B.D., Cox, K., Kakar, S., Gerstenfeld, L., Einhorn, T., Tabin, C.J., Rosen, V.: BMP2 activity, although dispensable for bone formation, is required for the initiation of fracture healing. Nat. Genet. **38**(12), 1424–1429 (2006). doi:10.1038/Ng1916
124. van der Eerden, B.C.J., Karperien, M., Wit, J.M.: Systemic and local regulation of the growth plate. Endocr. Rev. **24**(6), 782–801 (2003). doi:10.1210/Er.2002-0033
125. van Donkelaar, C.C., Huiskes, R.: The PTHrP-Ihh feedback loop in the embryonic growth plate allows PTHrP to control hypertrophy and Ihh to regulate proliferation. Biomech. Model. Mechanbiol. **6**(1–2), 55–62 (2007). doi:10.1007/s10237-006-0035-0
126. Vortkamp, A., Lee, K., Lanske, B., Segre, G.V., Kronenberg, H.M., Tabin, C.J.: Regulation of rate of cartilage differentiation by Indian hedgehog and PTH-related protein. Science **273**(5275), 613–622 (1996)
127. Williams, R.M., Zipfel, W.R., Tinsley, M.L., Farnum, C.E.: Solute transport in growth plate cartilage: in vitro and in vivo. Biophys. J. **93**(3), 1039–1050 (2007). doi:10.1529/biophysj.106.097675
128. Wood, B.D., Quintard, M., Whitaker, S.: Calculation of effective diffusivities for biofilms and tissues. Biotechnol. Bioeng. **77**(5), 495–516 (2002). 10.1002/bit.10075 [pii]
129. Wood, B.D., Whitaker, S.: Diffusion and reaction in biofilms. Chem. Eng. Sci. **53**(3), 397–425 (1998)
130. Zhou, S., Cui, Z., Urban, J.P.G.: Nutrient gradients in engineered cartilage: metabolic kinetics measurement and mass transfer modeling. Biotechnol. Bioeng. **101**(2), 408–421 (2008). doi:10.1002/Bit.21887